

Longitudinal wave-breaking limits in a unified geometric model of relativistic warm plasmas

DA Burton
 Department of Physics,
 Lancaster University, UK
 and The Cockcroft Institute, UK

A Noble
 Department of Physics,
 Lancaster University, UK
 and University of Strathclyde, UK

November 1, 2018

Abstract

The covariant Vlasov-Maxwell system is used to study breaking of relativistic warm plasma waves. The well-known theory of relativistic warm plasmas due to Katsouleas and Mori (KM) is subsumed within a unified geometric formulation of the ‘waterbag’ paradigm over spacetime. We calculate the maximum amplitude E_{\max} of non-linear longitudinal electric waves for a particular class of waterbags whose geometry is a simple 3-dimensional generalization (in velocity) of the 1-dimensional KM waterbag (in velocity). It is well known that the value of $\lim_{v \rightarrow c} E_{\max}$ (with the effective temperature of the plasma electrons held fixed) diverges for the KM model; however, we show that a certain class of simple 3-dimensional waterbags yields a finite value for $\lim_{v \rightarrow c} E_{\max}$, where v is the phase velocity of the wave and c is the speed of light.

Introduction

Considerable effort has been devoted to developing compact accelerators employing the enormous electric fields present in plasma wakes driven by intense lasers [1] or charged particle beams [2] (see [3,4] for recent discussions). Conventional accelerators operate by exciting RF microwave cavities with klystrons and use the longitudinal electric component of a cavity mode to accelerate bunches of charged particles for subsequent collision. However, it is anticipated that electric field strengths in the next generation of accelerators will be so high that the RF cavity walls may undergo electrical breakdown [5]. To address this issue, researchers have turned to plasma-based acceleration mechanisms whose field can be orders of magnitude beyond that of conventional accelerators. Recent years have seen the on-going development of *compact* sources of intense electromagnetic radiation in the X-ray to THz frequency range [6] that employ laser-driven plasma acceleration. Such sources promise a wide range of applications in medicine, material science and security.

A sufficiently short and intense laser pulse propagating through a plasma may create a travelling longitudinal plasma wave whose velocity is approximately the same as the laser pulse’s group velocity. However, it is not possible to sustain arbitrarily large electric fields; substantial numbers of plasma electrons become trapped in the wave and are accelerated, which dampens the wave. Indeed, the trapping phenomenon in longitudinal plasma waves lies at the heart of the original laser wakefield accelerator concept [1].

Although the evolution of a plasma wave dynamically trapping particles is complex, over the years much effort has been devoted to analytically understanding the upper bound (‘wave-breaking limit’) on the amplitude of plasma waves. Wave-breaking limits were first calculated for cold plasmas [7, 8] undergoing non-linear longitudinal electrostatic oscillations, and thermal effects were later included in non-relativistic [9] and relativistic [10–12] contexts. The results for the cold plasma are uncontroversial, but recent discussion [13–15] has uncovered difficulties with establishing an agreed analytical description of longitudinal wave-breaking in warm plasmas; in particular, it has been noted that different plasma models based on different assumptions yield different results. Models of non-linear plasma waves near breaking are approaching the limits of their domain of applicability, and different models exhibit different wave-breaking limits. Although recent experiments [16–18] operate in the 3-dimensional ‘bubble’ (or ‘blow-out’) regime [19] and exploit *transverse* wave-breaking [20], recent work [13–15] has rekindled interest in the theory of longitudinal wave-breaking.

Recent discussion [13–15] includes comparison of the behaviour of the relativistic ‘waterbag’ model [10, 21] due to Katsouleas and Mori (abbreviated as KM) and a warm plasma model [12] due to Schroeder, Esarey and

Shadwick (abbreviated as SES) employing velocity moments of the 1-particle plasma electron distribution. The KM and SES models yield different results for the maximum amplitude of non-linear electrostatic oscillations in the limit $v \rightarrow c$ with the temperature of the plasma held fixed (v is the phase velocity of the plasma wave with respect to the laboratory frame). The KM maximum electric field diverges logarithmically in $\gamma = 1/\sqrt{1 - v^2/c^2}$ as $v \rightarrow c$, whereas the SES maximum electric field tends to a finite value as $v \rightarrow c$ (with the initial plasma temperature held fixed in the limit $v \rightarrow c$). Employing velocity moments of the 1-particle plasma electron distribution, SES require that the distribution remains narrow in velocity spread whereas the KM approach employs a particular waterbag solution to the Vlasov equation. The disagreement of the two approaches has been attributed to the waterbag's piecewise constant structure and lack of a tail [14].

The KM model is formulated over 2-dimensional spacetime and SES employ a line distribution in longitudinal velocity to simplify their field equations on 4-dimensional spacetime. Neither model admits a plasma electron distribution with a non-vanishing transverse thermal spread. Thus, a theory of waterbags over 4-dimensional spacetime was recently developed [22, 23] to permit analytical investigation of wave-breaking as a function of the 3-dimensional shape (in velocity) of the plasma electron distribution. In the following we cast the KM field equations in a form comparable with those of the waterbag over 4-dimensional spacetime and, for the first time, give a unified presentation of the derivation of wave-breaking limits in the KM model and our waterbag model. We conclude with a comparison of the predictions of a particular class of our waterbags, the KM model and SES model. We find that the results of our present approach have more in common with the SES model than the KM model.

1 Vlasov-Maxwell equations

The brief summary of the Vlasov-Maxwell equations given below establishes our conventions; further details may be found in [23, 24]. We employ the Einstein summation convention throughout this article. Latin indices a, b, c run over 0, 1, 2, 3 and units are used in which the speed of light $c = 1$ and the permittivity of the vacuum $\epsilon_0 = 1$.

Let (x^a) be an inertial coordinate system on Minkowski spacetime (\mathcal{M}, g) where x^0 is the proper time of observers at fixed Cartesian coordinates (x^1, x^2, x^3) in the laboratory. The metric tensor g has the form

$$g = \eta_{ab} dx^a \otimes dx^b \quad (1)$$

where

$$\eta_{ab} = \begin{cases} -1 & \text{if } a = b = 0, \\ 1 & \text{if } a = b \neq 0, \\ 0 & \text{if } a \neq b. \end{cases} \quad (2)$$

Let (x^a, \dot{x}^b) be an induced coordinate system on the total space $T\mathcal{M}$ of the tangent bundle $(T\mathcal{M}, \Pi, \mathcal{M})$ and in the following, where convenient, we will write x instead of x^a and \dot{x} instead of \dot{x}^b . For notational simplicity, we will not distinguish between a point in a manifold and its coordinate representation.

The total space \mathcal{E} of the sub-bundle $(\mathcal{E}, \Pi|_{\mathcal{E}}, \mathcal{M})$ of $(T\mathcal{M}, \Pi, \mathcal{M})$ is the set of timelike, future-directed, unit normalized tangent vectors on \mathcal{M} ,

$$\mathcal{E} = \{(x, \dot{x}) \in T\mathcal{M} \mid \varphi = 0 \text{ and } \dot{x}^0 > 0\} \quad (3)$$

where

$$\varphi = \eta_{ab} \dot{x}^a \dot{x}^b + 1. \quad (4)$$

Plasma electrons are described statistically by a 1-particle distribution f on $T\mathcal{M}$ which induces a number 4-current vector field N ,

$$N = N^a \frac{\partial}{\partial x^a}, \quad (5)$$

$$N^a(x) = \int_{\mathcal{E}_x} \dot{x}^a f \iota_X \#1, \quad (6)$$

where $\mathcal{E}_x = (\Pi|_{\mathcal{E}})^{-1}(x)$ is the fibre of $(\mathcal{E}, \Pi|_{\mathcal{E}}, \mathcal{M})$ over $x \in \mathcal{M}$. The 3-form $\iota_X \#1$ on $T\mathcal{M}$ is induced from the 4-form $\#1$,

$$\#1 = dx^0 \wedge dx^1 \wedge dx^2 \wedge dx^3, \quad (7)$$

and the dilation vector field X ,

$$X = \dot{x}^a \frac{\partial}{\partial \dot{x}^a}, \quad (8)$$

on $T\mathcal{M}$, where ι_X is the interior product on forms. It may be shown

$$\iota_X \#1 \simeq \frac{1}{\sqrt{1 + |\dot{\mathbf{x}}|^2}} dx^1 \wedge dx^2 \wedge dx^3 \quad (9)$$

where $|\dot{\mathbf{x}}|^2 = (\dot{x}^1)^2 + (\dot{x}^2)^2 + (\dot{x}^3)^2$ and \simeq denotes equality under restriction to \mathcal{E} by pull-back. The above are specialised to inertial coordinates (x^a) on Minkowski spacetime; their form in a general coordinate system may be found in [23, 24].

We are interested in the evolution of a plasma over timescales during which the motion of the ions is negligible in comparison with the motion of the electrons. We assume that the ions are at rest and distributed homogeneously in the laboratory frame. Their worldlines are trajectories of the vector field $N_{\text{ion}} = n_{\text{ion}} \partial / \partial x^0$ on \mathcal{M} where n_{ion} is the ion number density (a positive definite constant) in the laboratory frame. The Maxwell equations are

$$dF = 0, \quad (10)$$

$$d \star F = -q \star \tilde{N} + q \star \tilde{N}_{\text{ion}} \quad (11)$$

where $F = \frac{1}{2} F_{ab} dx^a \wedge dx^b$ is the electromagnetic 2-form and q is the charge on the electron (with $q < 0$). The Hodge map \star is induced from (1) and the volume 4-form $\star 1$,

$$\star 1 = dx^0 \wedge dx^1 \wedge dx^2 \wedge dx^3, \quad (12)$$

on \mathcal{M} . The 1-forms \tilde{N} , \tilde{N}_{ion} are the metric duals of the vector fields N , N_{ion} respectively, i.e. the 1-form \tilde{Y} satisfies $\tilde{Y}(Z) = g(Y, Z)$ for all vector fields Z on \mathcal{M} .

The scalar field f satisfies the Vlasov equation, which may be written

$$\dot{x}^a \left(\frac{\partial f}{\partial x^a} - \frac{q}{m} F^b \mathbf{V}_a \frac{\partial f}{\partial \dot{x}^b} \right) \simeq 0 \quad (13)$$

on \mathcal{E} , where $F^b \mathbf{V}_a$ is the vertical lift of $F^b{}_a = \eta^{bc} F_{ca}$ from \mathcal{M} to $T\mathcal{M}$,

$$F^b \mathbf{V}_a(x, \dot{x}) = F^b{}_a(x), \quad (14)$$

and m is the electron rest mass.

The equations of motion for a waterbag distribution are readily motivated via a global expression of the local Vlasov equation (13). Introduce the Liouville vector field L ,

$$L = \dot{x}^a \left(\frac{\partial}{\partial x^a} - \frac{q}{m} F^b \mathbf{V}_a \frac{\partial}{\partial \dot{x}^b} \right), \quad (15)$$

on $T\mathcal{M}$ and the 6-form ω ,

$$\omega = \iota_L \iota_X (\star 1^{\mathbf{V}} \wedge \#1) \quad (16)$$

where the 4-form $\star 1^{\mathbf{V}}$,

$$\star 1^{\mathbf{V}} = dx^0 \wedge dx^1 \wedge dx^2 \wedge dx^3, \quad (17)$$

is the vertical lift of the spacetime volume 4-form $\star 1$ from \mathcal{M} to $T\mathcal{M}$. It can be shown

$$d\omega \simeq 0 \quad (18)$$

and the Vlasov equation (13) can be written

$$d(f\omega) \simeq 0. \quad (19)$$

Thus, it follows

$$\int_{\mathcal{B}} d(f\omega) = 0 \quad (20)$$

where \mathcal{B} is a 7-dimensional region in \mathcal{E} and using Stokes' theorem on forms (see, for example, [25,26]) we obtain

$$\int_{\partial\mathcal{B}} f\omega = 0 \quad (21)$$

where $\partial\mathcal{B}$ is the boundary of \mathcal{B} .

1.1 Waterbag distributions

We consider distributions for which $f = \alpha$ is a positive constant inside a 7-dimensional region $\mathcal{U} \subset \mathcal{E}$ and $f = 0$ outside. In particular, we consider \mathcal{U} to be the union over each point $x \in \mathcal{M}$ of a domain \mathcal{W}_x whose boundary $\partial\mathcal{W}_x$ in \mathcal{E} is topologically equivalent to the 2-sphere. Such piecewise constant distributions are called 'waterbags'.

Choosing \mathcal{B} in (21) to be a small 7-dimensional 'pill-box' that intersects $\partial\mathcal{W}_x$ and evaluating the integral in the limit as the 'height' of \mathcal{B} tends to zero, we recover a jump condition on $f\omega$ that leads to

$$d\lambda \wedge \omega \simeq 0 \text{ at } \lambda = 0 \quad (22)$$

where $\lambda = 0$ is the union over x of the boundaries $\partial\mathcal{W}_x$. If $\lambda = 0$ is the image of the embedding map Σ ,

$$\begin{aligned} \Sigma : \mathcal{M} \times S^2 &\rightarrow \mathcal{E} \\ (x, \xi) &\mapsto (x, \dot{x} = V_\xi(x)), \end{aligned} \quad (23)$$

where $\xi \in S^2$ has coordinates (ξ^1, ξ^2) , then it follows [23] from (8, 15, 16) that (22) is equivalent to

$$(\nabla_{V_\xi} \widetilde{V}_\xi - \frac{q}{m} \iota_{V_\xi} F) \wedge \Omega_\xi = 0. \quad (24)$$

Here, V_ξ and Ω_ξ are families of vector fields and 2-forms on \mathcal{M} respectively, where

$$V_\xi = V_\xi^a \frac{\partial}{\partial x^a}, \quad (25)$$

$$\Omega_\xi = \frac{\partial V_\xi^a}{\partial \xi^1} dx_a \wedge \frac{\partial V_\xi^b}{\partial \xi^2} dx_b. \quad (26)$$

with $dx_a = \eta_{ab} dx^b$. Note that since the image of Σ lies in \mathcal{E} it follows that, for each $\xi \in S^2$, V_ξ is timelike, unit normalized and future-directed:

$$g(V_\xi, V_\xi) = -1, \quad g(V_\xi, \frac{\partial}{\partial x^0}) < 0. \quad (27)$$

We adopt (24) as the equation of motion for the waterbag boundary $\partial\mathcal{W}_x$.

It may be shown that a particular class of solutions to (24) satisfies

$$F = \frac{m}{q} d\widetilde{V}_\xi \quad (28)$$

and using (11) we obtain the field equation

$$d \star d\widetilde{V}_\xi = -\frac{q^2}{m} (\star \widetilde{N} - \star \widetilde{N}_{\text{ion}}) \quad (29)$$

on \mathcal{M} with the condition that $d\widetilde{V}_\xi$ is independent of ξ . For simplicity, we have neglected the direct contribution of the driver (laser pulse or particle bunch) to the total electromagnetic field in (28).

For a discussion of solutions to (24) that do not satisfy (28) see [23].

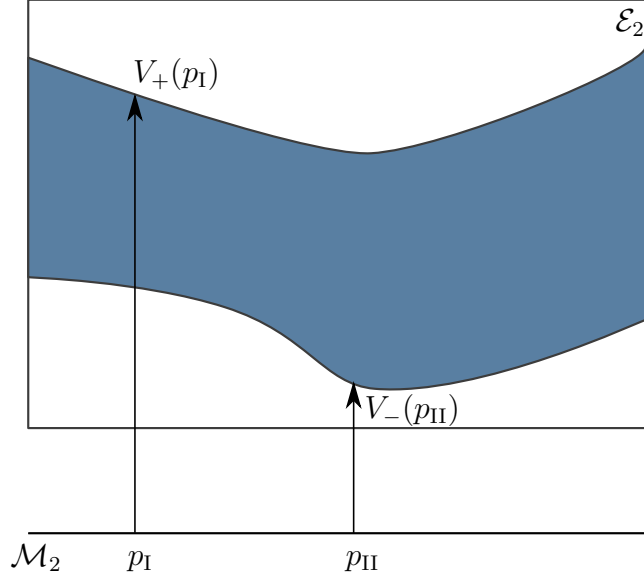


Figure 1: Illustration of a waterbag distribution over 2-dimensional spacetime \mathcal{M}_2 with $p_I = (t_I, z_I)$ and $p_{II} = (t_{II}, z_{II})$. The shaded region is the interior of the waterbag (where f is non-zero), and the 2-vector fields $\{V_+, V_-\}$ determine the boundary of the waterbag.

2 Electrostatic oscillations on 2-dimensional spacetime

Before analysing (27, 29) further it is useful to briefly discuss their analogue on 2-dimensional spacetime for facilitating comparison with the approach adopted in [10,21]. Although formulated on 4-dimensional spacetime, equations (27, 29) have a similar structure for any number of dimensions. In particular, we now consider 2-dimensional Minkowski spacetime (\mathcal{M}_2, g)

$$g = -dt \otimes dt + dz \otimes dz, \quad (30)$$

$$\star 1 = dt \wedge dz \quad (31)$$

where $(t, z)^1$ is a Cartesian coordinate system in the laboratory inertial frame. An induced coordinate system on $T\mathcal{M}_2$ is (t, z, \dot{t}, \dot{z}) and the 2-form $\#1$ and dilation vector field X over $T\mathcal{M}_2$ are

$$\#1 = d\dot{t} \wedge d\dot{z}, \quad (32)$$

$$X = \dot{t} \frac{\partial}{\partial \dot{t}} + \dot{z} \frac{\partial}{\partial \dot{z}}. \quad (33)$$

Furthermore, ξ is now an element of the 0-sphere $\{+, -\}$ and $\Omega_\xi = 1$ is a constant 0-form. Thus, the analogue to (24) is

$$\nabla_{V_+} \widetilde{V}_+ - \frac{q}{m} \iota_{V_+} F = 0, \quad (34)$$

$$\nabla_{V_-} \widetilde{V}_- - \frac{q}{m} \iota_{V_-} F = 0, \quad (35)$$

where $\{V_+, V_-\}$ satisfy the conditions

$$g(V_+, V_+) = -1, \quad g(V_+, \frac{\partial}{\partial t}) < 0, \quad (36)$$

$$g(V_-, V_-) = -1, \quad g(V_-, \frac{\partial}{\partial t}) < 0, \quad (37)$$

and the only non-trivial Maxwell equation for the 2-form F is

$$d \star F = -q \star \widetilde{N} + q \star \widetilde{N}_{\text{ion}} \quad (38)$$

¹We use (t, z) rather than (x^a) to distinguish coordinates on 2- and 4-dimensional spacetimes.

where $N_{\text{ion}} = n_{\text{ion}}\partial/\partial t$ is the ion number 2-current and $F = Edt \wedge dz$ where E is the electric field along the z -axis.

On the unit hyperbola bundle \mathcal{E}_2 , $t = \sqrt{1 + \dot{z}^2}$ and the components of the electron number 2-current $N = N^t\partial/\partial t + N^z\partial/\partial z$ corresponding to (6) are

$$\begin{aligned} N^t &= \int_{\mathbb{R}} f(t, z, \dot{t}, \dot{z}) d\dot{z} = \alpha(Y_+ - Y_-), \\ N^z &= \int_{\mathbb{R}} \frac{\dot{z}}{\sqrt{1 + \dot{z}^2}} f(t, z, \dot{t}, \dot{z}) d\dot{z} = \alpha\left(\sqrt{1 + Y_+^2} - \sqrt{1 + Y_-^2}\right), \end{aligned} \quad (39)$$

where

$$f = \begin{cases} \alpha, & Y_- \leq \dot{z} \leq Y_+, \\ 0, & \dot{z} < Y_- \text{ or } \dot{z} > Y_+ \end{cases} \quad (40)$$

with α a positive non-zero constant and $\{Y_+, Y_-\}$ 0-forms on \mathcal{M}_2 . The 2-velocity fields $\{V_+, V_-\}$ satisfy

$$V_{\pm} = \sqrt{1 + Y_{\pm}^2} \frac{\partial}{\partial t} + Y_{\pm} \frac{\partial}{\partial z} \quad (41)$$

and it follows

$$\tilde{N} = \alpha \star (\tilde{V}_+ - \tilde{V}_-). \quad (42)$$

See figure 1.

Unlike their 4-dimensional analogue, which may include transverse electromagnetic fields, (34,35) are *uniquely*² solved by

$$d\tilde{V}_{\pm} = \frac{q}{m} F \quad (43)$$

and using (38) it follows

$$d \star d\tilde{V}_{\pm} = -\frac{q^2}{m} (\star \tilde{N} - \star \tilde{N}_{\text{ion}}) \quad (44)$$

subject to the condition $d\tilde{V}_+ = d\tilde{V}_-$.

Alternatively, one may follow the approach adopted in [10] by casting the above as a warm fluid. The type (0, 2) stress-energy-momentum tensor $\mathcal{T}_{\text{fluid}}$ of the electron fluid is

$$\mathcal{T}_{\text{fluid}} = \left(m \int_{\mathbb{R}} \frac{\dot{z}^{\mu} \dot{z}^{\nu} f}{\sqrt{1 + \dot{z}^2}} d\dot{z} \right) \frac{\partial}{\partial z^{\mu}} \otimes \frac{\partial}{\partial z^{\nu}} \quad (45)$$

where Greek indices μ, ν run over 0, 1 and $z^0 = t$, $z^1 = z$, $\dot{z}^0 = \sqrt{1 + \dot{z}^2}$, $\dot{z}^1 = \dot{z}$. It can be shown that $\mathcal{T}_{\text{fluid}}$ induced by the above waterbag distribution can be expressed entirely in terms of the proper number density n of the electron fluid, the electron fluid's bulk 2-velocity U and the spacetime metric:

$$\mathcal{T}_{\text{fluid}} = (\rho + p)U \otimes U + p\tilde{g} \quad (46)$$

where \tilde{g} is the inverse metric tensor

$$\tilde{g} = -\frac{\partial}{\partial t} \otimes \frac{\partial}{\partial t} + \frac{\partial}{\partial z} \otimes \frac{\partial}{\partial z} \quad (47)$$

and

$$U = \frac{1}{\sqrt{-g(Z, Z)}} Z, \quad Z = \frac{1}{2}(V_+ + V_-), \quad (48)$$

$$N = nU, \quad n = \sqrt{-g(N, N)}, \quad (49)$$

²Proper incorporation of transverse fields requires at least 2 spatial dimensions.

with the equations of state

$$\rho = m\alpha \left[\frac{n}{2\alpha} \sqrt{1 + \left(\frac{n}{2\alpha}\right)^2} + \sinh^{-1}\left(\frac{n}{2\alpha}\right) \right], \quad (50)$$

$$p = m\alpha \left[\frac{n}{2\alpha} \sqrt{1 + \left(\frac{n}{2\alpha}\right)^2} - \sinh^{-1}\left(\frac{n}{2\alpha}\right) \right]. \quad (51)$$

The equation of motion of the electron fluid,

$$(\rho + p)\nabla_U \tilde{U} = qn\iota_U F - \iota_U(dp \wedge \tilde{U}), \quad (52)$$

follows from the zero divergence of the sum of $\mathcal{T}_{\text{fluid}}$ and the Maxwell stress-energy-momentum tensor where

$$g(U, U) = -1, \quad g(U, \frac{\partial}{\partial t}) < 0. \quad (53)$$

It should be stressed that the warm fluid model (50, 51, 52) is equivalent to (34, 35, 36, 37). Thus, (34, 35, 36, 37) may be replaced by an equivalent field theory expressed in terms of a finite set of moments of f on 2-dimensional spacetime. However, the situation is more complicated for waterbags over 4-dimensional spacetime where second, and higher, order moments of f in \dot{x} are not, in general, easily expressible in terms of zeroth and first order moments of f . In general, the moment hierarchy does not automatically close.

We will now obtain a non-linear ordinary differential equation describing 1-dimensional electrostatic oscillations and determine an expression for the wave-breaking limit of this model. Derivation of wave-breaking limits starting from $\mathcal{T}_{\text{fluid}}$ and the equations of state (50, 51) may be found in [10, 21]. However, we will work directly with (36, 37, 42, 44) to facilitate comparison with our model on 4-dimensional spacetime.

Let all field components with respect to the laboratory frame (dt, dz) be functions of $\zeta = z - vt$ only (the ‘quasi-static assumption’), where $0 < v < 1$, and let (e^1, e^2) be the basis

$$e^1 = vdz - dt, \quad e^2 = dz - vdt. \quad (54)$$

The coframe $(\gamma e^1, \gamma e^2)$ is an orthonormal basis adapted to observers moving at velocity v along z (i.e observers in the ‘wave frame’) where $\gamma = (1 - v^2)^{-1/2}$ is the Lorentz factor of such observers relative to the laboratory. So, $\gamma e^2(N_{\text{ion}}) = -\gamma n_{\text{ion}}v$ is the component of the ion number 1-current in the wave frame.

In the basis (e^1, e^2) , \tilde{V}_{\pm} can be decomposed as

$$\tilde{V}_{\pm} = (\mu(\zeta) + A_{\pm})e^1 + \psi_{\pm}(\zeta)e^2 \quad (55)$$

where $\{A_+, A_-\}$ are constant. Note that this is the most general decomposition compatible with equation (43) and the quasi-static assumption.

Solving (36, 37) for ψ_{\pm}^2 gives

$$\psi_{\pm}^2 = (\mu + A_{\pm})^2 - \gamma^2 \quad (56)$$

and additional physical information is needed to fix the sign of ψ_{\pm} . Here, we demand that all electrons described by the waterbag are travelling slower than the wave so $\psi_{\pm} = -\sqrt{(\mu + A_{\pm})^2 - \gamma^2}$ and (55) is

$$\tilde{V}_{\pm} = (\mu + A_{\pm})e^1 - \left((\mu + A_{\pm})^2 - \gamma^2 \right)^{1/2} e^2. \quad (57)$$

Substituting (55) into equation (43) yields

$$E = \frac{1}{\gamma^2} \frac{m}{q} \frac{d\mu}{d\zeta}, \quad (58)$$

and equation (44) yields the nonlinear oscillator equation

$$\frac{1}{\gamma^2} \frac{d^2\mu}{d\zeta^2} = -\frac{q^2}{m} \gamma^2 n_{\text{ion}} - \frac{q^2}{m} \alpha \left[\sqrt{(\mu + A_+)^2 - \gamma^2} - \sqrt{(\mu + A_-)^2 - \gamma^2} \right] \quad (59)$$

with the algebraic constraint

$$A_+ - A_- = -\frac{n_{\text{ion}}\gamma^2 v}{\alpha} < 0. \quad (60)$$

2.1 Electrostatic wave-breaking

In the wave frame the relativistic energies of the two ends of the waterbag are $m(\mu + A_+)/\gamma$ and $m(\mu + A_-)/\gamma$ respectively, and since $m(\mu + A_+)/\gamma \geq m$ it follows $\mu + A_{\pm} \geq \gamma$. Using (60), $\mu + A_- > \mu + A_+$ and hence $\mu + A_+ \geq \gamma$ implies $\mu + A_- > \gamma$. Thus, $\mu + A_{\pm} \geq \gamma$ may be reduced to $\mu \geq \mu_{\text{wb}}$ where

$$\mu_{\text{wb}} = -A_+ + \gamma. \quad (61)$$

Alternatively, one may arrive at the same conclusion by inspecting the right-hand side of (59) and using $\mu + A_{\pm} > 0$ (which follows because V_+ and V_- are future-pointing). Thus, there is an upper bound on the amplitude of oscillatory solutions to (59), which leads to an upper bound E_{max} on the electric field E (the ‘wave-breaking limit’ of this model).

During an oscillation E vanishes when $d\mu/d\zeta$ vanishes and $|E|$ is at a maximum when $|d\mu/d\zeta|$ is at a maximum (see (58) and note $q < 0$). A maximum of $|d\mu/d\zeta|$ occurs at values ζ_0 of ζ where $\mu(\zeta_0)$ equals the oscillator equilibrium μ_{eq} . Furthermore, for the maximum amplitude oscillation $d\mu/d\zeta$ vanishes when $\mu = \mu_{\text{wb}}$. An upper bound E_{max} on the magnitude $|E|$ of the electric field is obtained by evaluating the first integral of (59) between $\mu = \mu_{\text{wb}}$ and $\mu = \mu_{\text{eq}}$.

Without loss of generality, we can choose the split between μ and A_{\pm} such that

$$A_+ = -A_- = -a, \quad a = \frac{n_{\text{ion}}\gamma^2 v}{2\alpha}. \quad (62)$$

Using (58, 59) it follows

$$E_{\text{max}}^2 = 2mn_{\text{ion}} \left[-\mu_{\text{eq}} + \mu_{\text{wb}} + \frac{1}{2} \frac{v}{a} \int_{\mu_{\text{wb}}}^{\mu_{\text{eq}}} \left(\sqrt{[\mu + a]^2 - \gamma^2} - \sqrt{[\mu - a]^2 - \gamma^2} \right) d\mu \right] \quad (63)$$

where μ_{eq} is the equilibrium solution to (59), which satisfies

$$\frac{2a}{v} = \sqrt{(\mu_{\text{eq}} + a)^2 - \gamma^2} - \sqrt{(\mu_{\text{eq}} - a)^2 - \gamma^2}. \quad (64)$$

The constant a is fixed in terms of an effective temperature T_{eq} associated with the oscillator equilibrium μ_{eq} . Noting that $n = n_{\text{ion}}$ when the waterbag is in its equilibrium state ($\mu = \mu_{\text{eq}}$), and assuming $n_{\text{ion}} \ll 2\alpha$ in (51) it follows

$$p_{\text{eq}} \approx \frac{mn_{\text{ion}}^3}{3(2\alpha)^2}. \quad (65)$$

Introducing T_{eq} via $p_{\text{eq}} = n_{\text{ion}}k_B T_{\text{eq}}$, where k_B is Boltzmann’s constant, we find

$$\frac{n_{\text{ion}}}{2\alpha} \approx \sqrt{\frac{3k_B T_{\text{eq}}}{m}}, \quad a \approx \gamma^2 v \sqrt{\frac{3k_B T_{\text{eq}}}{m}} \quad (66)$$

where (62) has been used. Hence, $n_{\text{ion}} \ll 2\alpha$ means that the thermal energy of the electron fluid in the oscillator equilibrium state is much less than the rest mass-energy of the electron.

The wave-breaking limit E_{max} can be readily analysed for $\gamma \gg 1$ via asymptotic approximation in a small parameter ε ,

$$\varepsilon = \frac{\gamma}{a} = \frac{2\alpha}{n_{\text{ion}}v} \frac{1}{\gamma}, \quad (67)$$

where (62) has been used. Employing (61, 63, 64) it follows

$$E_{\text{max}}^2 = 2mn_{\text{ion}}a \left[-\hat{\mu}_{\text{eq}} + \hat{\mu}_{\text{wb}} + \frac{1}{2} v \int_{\hat{\mu}_{\text{wb}}}^{\hat{\mu}_{\text{eq}}} \left(\sqrt{[\hat{\mu} + 1]^2 - \varepsilon^2} - \sqrt{[\hat{\mu} - 1]^2 - \varepsilon^2} \right) d\hat{\mu} \right], \quad (68)$$

$$\frac{1}{2} v \left(\sqrt{[\hat{\mu}_{\text{eq}} + 1]^2 - \varepsilon^2} - \sqrt{[\hat{\mu}_{\text{eq}} - 1]^2 - \varepsilon^2} \right) = 1, \quad (69)$$

$$\hat{\mu}_{\text{wb}} = 1 + \varepsilon \quad (70)$$

where, $\hat{\mu} = \mu/a$. To proceed further, we express v in (68, 69) as a function of ε and a parameter b that characterizes the effective temperature of the oscillator equilibrium distribution. Using (62, 67) it follows

$$v = \frac{1}{\sqrt{1 + \varepsilon^2 b^2}}, \quad (71)$$

where b is

$$b = \frac{n_{\text{ion}}}{2\alpha}. \quad (72)$$

The dominant ε dependence (as $\varepsilon \rightarrow 0$ with b held fixed) of E_{max}^2 arises from the second term in the integrand in (68) and may be extracted by expanding the integrand with respect to ε and integrating each summand over $\hat{\mu}$. Since, for $\nu > \varepsilon > 0$,

$$\sqrt{\nu^2 - \varepsilon^2} = \nu - \frac{1}{2} \frac{\varepsilon^2}{\nu} + \sum_{n=2}^{\infty} c_n \frac{\varepsilon^{2n}}{\nu^{2n-1}} \quad (73)$$

where c_n are constants, and inspection of (69) reveals

$$\hat{\mu}_{\text{eq}} = h(\varepsilon^2) = h(0) + h'(0)\varepsilon^2 + \mathcal{O}(\varepsilon^4) \quad (\varepsilon \rightarrow 0), \quad (74)$$

we find, for $h(0) \gg 1$,

$$\begin{aligned} \int_{\hat{\mu}_{\text{wb}}}^{\hat{\mu}_{\text{eq}}} \sqrt{[\hat{\mu} - 1]^2 - \varepsilon^2} d\hat{\mu} &= \left(\frac{1}{2} [\hat{\mu} - 1]^2 - \frac{1}{2} \varepsilon^2 \ln(\hat{\mu} - 1) \right) \Big|_{\hat{\mu}_{\text{wb}}}^{\hat{\mu}_{\text{eq}}} + \sum_{n=2}^{\infty} c_n \frac{1}{2 - 2n} \left(\frac{\varepsilon^{2n}}{[\hat{\mu}_{\text{eq}} - 1]^{2n-2}} - \varepsilon^2 \right) \\ &= \frac{1}{2} [\hat{\mu} - 1]^2 \Big|_{\hat{\mu}_{\text{wb}}}^{\hat{\mu}_{\text{eq}}} + \frac{1}{2} \varepsilon^2 \ln(\varepsilon) + \mathcal{O}(\varepsilon^2) \quad (\varepsilon \rightarrow 0) \end{aligned} \quad (75)$$

where (70) has been used. Furthermore, it follows from (69) that an asymptotic approximation for $h(0)$ in small b leads to

$$h(0) = \frac{1}{b} + \mathcal{O}(1) \quad (b \rightarrow 0). \quad (76)$$

Thus, (68) yields

$$\frac{E_{\text{max}}^2}{a} \approx -\frac{1}{2} m n_{\text{ion}} \varepsilon^2 \ln(\varepsilon) \quad (77)$$

for $\varepsilon, b \ll 1$. Introducing the effective temperature T_{eq} using (62, 66, 67) and noting $v \approx 1$, we obtain

$$E_{\text{max}}^2 \approx \frac{1}{2} \frac{m^2 c^2 \omega_p^2}{q^2} \sqrt{\frac{m c^2}{3 k_B T_{\text{eq}}}} \ln \left(\gamma \sqrt{\frac{3 k_B T_{\text{eq}}}{m c^2}} \right), \quad \varepsilon, b \ll 1 \quad (78)$$

where $\omega_p = \sqrt{n_{\text{ion}} q^2 / (m \varepsilon_0)}$ is the plasma frequency and the speed of light c and permittivity of the vacuum ε_0 have been restored. Equation (78) was obtained as a lower bound on E_{max}^2 in [13].

3 Longitudinal electrostatic oscillations on 4-dimensional spacetime

We now consider longitudinal electrostatic waves on 4-dimensional spacetime by closely following the above description on 2-dimensional spacetime.

As before, we adopt the ‘quasi-static assumption’. We seek a waterbag \mathcal{W}_x axisymmetric about \dot{x}^3 whose pointwise dependence in Minkowski spacetime \mathcal{M} is on the wave’s phase $\zeta = x^3 - v x^0$ only, where $0 < v < 1$. As before, the following results are applicable only if the longitudinal component of V_{ξ} in the wave frame is negative (no electron described by \mathcal{W}_x is moving faster along x^3 than the wave).

Decompose \tilde{V}_{ξ} in the wave frame as

$$\tilde{V}_{\xi} = [\mu(\zeta) + A(\xi^1)] e^1 + \psi(\xi^1, \zeta) e^2 + R \sin(\xi^1) \cos(\xi^2) dx^1 + R \sin(\xi^1) \sin(\xi^2) dx^2 \quad (79)$$

for $0 < \xi^1 < \pi$, $0 \leq \xi^2 < 2\pi$ where $R > 0$ is constant and

$$e^1 = vdx^3 - dx^0, \quad e^2 = dx^3 - vdx^0. \quad (80)$$

Here, $(\gamma e^1, \gamma e^2, dx^1, dx^2)$ is an orthonormal basis adapted to the wave frame, with $\gamma = 1/\sqrt{1-v^2}$. In the wave frame the relativistic energy of $P_\xi = mV_\xi$ is $m(\mu + A(\xi^1))/\gamma$ and it follows that $\mu + A(\xi^1) > 0$. Furthermore, using (27, 79) it follows

$$\psi = -\sqrt{[\mu + A(\xi^1)]^2 - \gamma^2[1 + R^2 \sin^2(\xi^1)]}, \quad (81)$$

where the negative square root is chosen because no electron is moving faster along x^3 than the wave, and we obtain

$$\mu \geq -A(\xi^1) + \gamma\sqrt{1 + R^2 \sin^2(\xi^1)}. \quad (82)$$

Substituting (79) into equation (28) leads to

$$F = \frac{m}{q} \frac{d\mu}{d\xi} e^2 \wedge e^1, \quad (83)$$

and (6, 29, 79, 81) yield

$$\frac{1}{\gamma^2} \frac{d^2\mu}{d\xi^2} = -\frac{q^2}{m} n_{\text{ion}} \gamma^2 - \frac{q^2}{m} 2\pi R^2 \alpha \int_0^\pi \left([\mu + A(\xi^1)]^2 - \gamma^2[1 + R^2 \sin^2(\xi^1)] \right)^{1/2} \sin(\xi^1) \cos(\xi^1) d\xi^1 \quad (84)$$

(c.f. equation (59)) and

$$2\pi R^2 \int_0^\pi A(\xi^1) \sin(\xi^1) \cos(\xi^1) d\xi^1 = -\frac{n_{\text{ion}} \gamma^2 v}{\alpha} \quad (85)$$

(c.f. equation (60)) where $\alpha > 0$ is the value of f inside \mathcal{W}_x .

The form of the 2nd order autonomous non-linear ordinary differential equation (84) for μ is fixed by specifying the generator $A(\xi^1)$ of $\partial\mathcal{W}_x$ subject to the normalization condition (85).

3.1 Electrostatic wave-breaking

The form of the integrand in (84) ensures that the magnitude of oscillatory solutions to (84) cannot be arbitrarily large. For our model, the wave-breaking value μ_{wb} is the largest μ for which the argument of the square root in (84) vanishes,

$$\mu_{\text{wb}} = \max \left\{ -A(\xi^1) + \gamma\sqrt{1 + R^2 \sin^2(\xi^1)} \mid 0 \leq \xi^1 \leq \pi \right\}, \quad (86)$$

because $\mu < \mu_{\text{wb}}$ yields an imaginary integrand in (84) for some ξ^1 .

The electric field has only one non-zero component E (in the x^3 direction). Using $F = E dx^0 \wedge dx^3$ and (80, 83) it follows

$$E = \frac{m}{q} \frac{1}{\gamma^2} \frac{d\mu}{d\xi} \quad (87)$$

and the wave-breaking limit E_{max} is obtained by evaluating the first integral of (84) between μ_{wb} where E vanishes and the oscillator equilibrium μ_{eq} of μ where $|E|$ is at a maximum. Using (85) to eliminate α it follows that μ_{eq} satisfies

$$\frac{1}{v} \int_0^\pi A(\xi^1) \sin(\xi^1) \cos(\xi^1) d\xi^1 = \int_0^\pi \left([\mu_{\text{eq}} + A(\xi^1)]^2 - \gamma^2[1 + R^2 \sin^2(\xi^1)] \right)^{1/2} \sin(\xi^1) \cos(\xi^1) d\xi^1 \quad (88)$$

with

$$\int_0^\pi A(\xi^1) \sin(\xi^1) \cos(\xi^1) d\xi^1 < 0 \quad (89)$$

since $\alpha, v > 0$. Equation (84) yields the maximum value E_{\max} of E ,

$$E_{\max}^2 = 2mn_{\text{ion}} \left[-\mu_{\text{eq}} + \mu_{\text{wb}} + \frac{v}{\int_0^\pi A(\xi^{1'}) \sin(\xi^{1'}) \cos(\xi^{1'}) d\xi^{1'}} \times \int_{\mu_{\text{wb}}}^{\mu_{\text{eq}}} \int_0^\pi \left([\mu + A(\xi^1)]^2 - \gamma^2 [1 + R^2 \sin^2(\xi^1)] \right)^{1/2} \sin(\xi^1) \cos(\xi^1) d\xi^1 d\mu \right]. \quad (90)$$

To proceed further we need to choose the generator $A(\xi^1)$ of the waterbag distribution. It turns out that even the simple choice

$$A(\xi^1) = -a \cos(\xi^1) \quad (91)$$

for $A(\xi^1)$, where a is a positive constant, leads to a wave-breaking limit E_{\max} with interesting behaviour, as we now show.

Using (90) it follows

$$E_{\max}^2 = 2mn_{\text{ion}} \left[-\mu_{\text{eq}} + \mu_{\text{wb}} + \frac{3v}{2a} \int_{\mu_{\text{wb}}}^{\mu_{\text{eq}}} \int_{-1}^1 \left([\mu + a\chi]^2 - \gamma^2 [1 + R^2(1 - \chi^2)] \right)^{1/2} \chi d\chi d\mu \right] \quad (92)$$

where $\chi = -\cos(\xi^1)$, equation (88) yields

$$\frac{3v}{2a} \int_{-1}^1 \left([\mu_{\text{eq}} + a\chi]^2 - \gamma^2 [1 + R^2(1 - \chi^2)] \right)^{1/2} \chi d\chi = 1 \quad (93)$$

and equation (86) may be written

$$\mu_{\text{wb}} = \max \left\{ -a\chi + \gamma \sqrt{1 + R^2(1 - \chi^2)} \mid -1 \leq \chi \leq 1 \right\}. \quad (94)$$

Examination of (94) reveals that two classes of waterbag arise according to whether or not the function

$$\chi \mapsto -a\chi + \gamma \sqrt{1 + R^2(1 - \chi^2)} \quad (95)$$

has a turning point in the interval $[-1, 1]$. Examples of the two classes are shown in figures 2 and 3. In each case, the plasma wave breaks when the uppermost part of the distribution achieves the phase velocity of the plasma wave (i.e. the longitudinal component ψ of V_ξ in the wave frame vanishes). Wave-breaking limits for the class in figure 2 have been calculated previously [22, 23] and here we focus on waterbags of the type shown in figure 3.

3.1.1 Calculation of the maximum electric field

The parameters a, R, γ are chosen to satisfy

$$\frac{a}{R} \sqrt{\frac{1 + R^2}{a^2 + \gamma^2 R^2}} > 1, \quad (96)$$

ensuring that (95) does not have a turning point in the interval $[-1, 1]$. Hence, the wave breaks when the tip $\chi = -\cos(0) = -1$ of the waterbag achieves the phase velocity of the plasma wave. Using (94) it follows

$$\mu_{\text{wb}} = a + \gamma \quad (97)$$

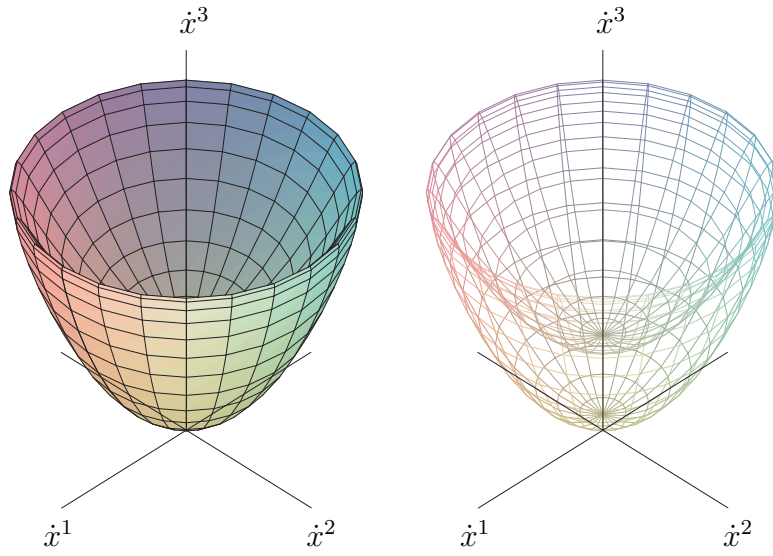


Figure 2: Two illustrations of the 4-velocity dependence of a particular ‘bowl’ waterbag. The axis of symmetry is aligned along \dot{x}^3 . The maximum electric field amplitude is achieved during the oscillation in which the top of the waterbag (a circle) grazes the phase speed of the wave.

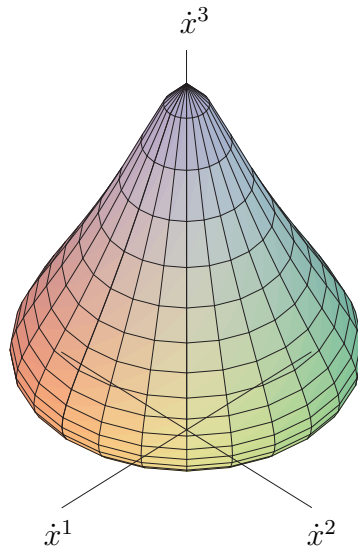


Figure 3: An illustration of the 4-velocity dependence of a particular ‘gourd’ waterbag. The axis of symmetry is aligned along \dot{x}^3 . The maximum electric field amplitude is achieved during the oscillation in which the tip of the waterbag grazes the phase speed of the wave.

which is formally identical to the wave-breaking limit of μ for the waterbag over 2-dimensional spacetime. This is quite different from the value of μ_{wb} for waterbags of the type shown in figure 2 (see [22, 23]).

Following a similar method to that used in section 2, we now evaluate (92) for $\gamma \gg 1$. Introducing $\hat{\mu} = \mu/a$ in (92, 93, 97) leads to

$$E_{\text{max}}^2 = 2mn_{\text{ion}}a \left[-\hat{\mu}_{\text{eq}} + \hat{\mu}_{\text{wb}} + \frac{3}{2}v \int_{\hat{\mu}_{\text{wb}}}^{\hat{\mu}_{\text{eq}}} \int_{-1}^1 \left([\hat{\mu} + \chi]^2 - \varepsilon^2[1 + R^2(1 - \chi^2)] \right)^{1/2} \chi d\hat{\mu} d\chi \right], \quad (98)$$

$$\frac{3}{2}v \int_{-1}^1 \left([\hat{\mu}_{\text{eq}} + \chi]^2 - \varepsilon^2[1 + R^2(1 - \chi^2)] \right)^{1/2} \chi d\chi = 1, \quad (99)$$

$$\hat{\mu}_{\text{wb}} = 1 + \varepsilon, \quad (100)$$

where, using (85),

$$a = \frac{3n_{\text{ion}}\gamma^2 v}{4\pi R^2 \alpha} \quad (101)$$

$$\varepsilon = \frac{\gamma}{a} = \frac{4\pi R^2 \alpha}{3n_{\text{ion}}\gamma v}. \quad (102)$$

Thus, it follows $\varepsilon \rightarrow 0$ as $v \rightarrow 1$ and we determine an asymptotic approximation for E_{max} in ε as $\varepsilon \rightarrow 0$.

Expansion in ε of the integrand in (98) yields

$$\left([\hat{\mu} + \chi]^2 - \varepsilon^2[1 + R^2(1 - \chi^2)] \right)^{1/2} = \hat{\mu} + \chi - \frac{1 + R^2(1 - \chi^2)}{2(\hat{\mu} + \chi)}\varepsilon^2 + \sum_{n=2}^{\infty} c_n \frac{(1 + R^2(1 - \chi^2))^n}{(\hat{\mu} + \chi)^{2n-1}}\varepsilon^{2n} \quad (103)$$

where the c_n are numerical constants. Using (103), the integral over $\hat{\mu}$ in (98) leads to a summand proportional to

$$f_n = \int_{-1}^1 \left[\frac{(1 + R^2(1 - \chi^2))^n}{(\hat{\mu}_{\text{eq}} + \chi)^{2n-2}} - \frac{(1 + R^2(1 - \chi^2))^n}{(1 + \varepsilon + \chi)^{2n-2}} \right] \chi d\chi, \quad n \geq 2 \quad (104)$$

where (100) has been used.

Inspection of (99) suggests an approximation for $\hat{\mu}_{\text{eq}}(\varepsilon)$ of the form

$$\hat{\mu}_{\text{eq}}(\varepsilon) = h(\varepsilon^2) = h(0) + h'(0)\varepsilon^2 + \mathcal{O}(\varepsilon^4) \quad (\varepsilon \rightarrow 0). \quad (105)$$

Using (102) it follows

$$v = \frac{1}{\sqrt{1 + \varepsilon^2 b^2}} = 1 - \frac{1}{2}\varepsilon^2 b^2 + \mathcal{O}(\varepsilon^4) \quad (\varepsilon \rightarrow 0), \quad (106)$$

$$b = \frac{3n_{\text{ion}}}{4\pi R^2 \alpha} = \frac{a}{\gamma^2 v} \quad (107)$$

and (99) leads to

$$-\frac{3}{2} \int_{-1}^1 \frac{1 + R^2(1 - \chi^2)}{\hat{\mu}_{\text{eq}}(0) + \chi} \chi d\chi = b^2. \quad (108)$$

Thus, $\hat{\mu}_{\text{eq}}(0)$ may be approximated as

$$\hat{\mu}_{\text{eq}}(0) = \frac{1}{b} \sqrt{1 + \frac{2R^2}{5}} + \mathcal{O}(1) \quad (b \rightarrow 0). \quad (109)$$

Repeated integration by parts in (104) leads to

$$f_n = \mathcal{O}(\varepsilon^{3-2n}) \quad (\varepsilon \rightarrow 0), \quad n \geq 2 \quad (110)$$

and we obtain the asymptotic approximation

$$\begin{aligned}
& \int_{-1}^1 \int_{1+\varepsilon}^{\hat{\mu}_{\text{eq}}} \left([\hat{\mu} + \chi]^2 - \varepsilon^2 [1 + R^2(1 - \chi^2)] \right)^{1/2} \chi d\chi d\hat{\mu} \\
&= \frac{2}{3}(\hat{\mu}_{\text{eq}} - \hat{\mu}_{\text{wb}}) - \frac{1}{2}\varepsilon^2 \int_{-1}^1 [1 + R^2(1 - \chi^2)] \ln \left(\frac{\hat{\mu}_{\text{eq}} + \chi}{\hat{\mu}_{\text{wb}} + \chi} \right) \chi d\chi + \mathcal{O}(\varepsilon^3) \quad (\varepsilon \rightarrow 0) \\
&= \frac{2}{3}(\hat{\mu}_{\text{eq}} - \hat{\mu}_{\text{wb}}) - \frac{1}{2}\varepsilon^2 \int_{-1}^1 [1 + R^2(1 - \chi^2)] \ln \left(\frac{\hat{\mu}_{\text{eq}}(0) + \chi}{1 + \chi} \right) \chi d\chi + \mathcal{O}(\varepsilon^3 \ln \varepsilon) \quad (\varepsilon \rightarrow 0).
\end{aligned} \tag{111}$$

Thus

$$\frac{E_{\text{max}}^2}{a} = mn_{\text{ion}}\varepsilon^2 \left\{ b^2(1 - \hat{\mu}_{\text{eq}}(0)) + \frac{3}{2} \int_{-1}^1 [1 + R^2(1 - \chi^2)] \ln \left(\frac{1 + \chi}{\hat{\mu}_{\text{eq}}(0) + \chi} \right) \chi d\chi \right\} + \mathcal{O}(\varepsilon^3 \ln \varepsilon) \quad (\varepsilon \rightarrow 0) \tag{112}$$

and retaining lowest order terms in ε , b , R yields

$$\begin{aligned}
E_{\text{max}}^2 &\approx \frac{3}{2} mn_{\text{ion}} a \varepsilon^2 \int_{-1}^1 [1 + R^2(1 - \chi^2)] \ln(1 + \chi) \chi d\chi, \\
&= 2\pi\alpha m R^2 \left(1 + \frac{1}{3} R^2 \right) \\
&\approx \frac{3}{2} mn_{\text{ion}} \frac{1}{b}
\end{aligned} \tag{113}$$

where (107) has been used to eliminate αR^2 .

Numerical validity of the above approximation is supported by figure 4. The solid curves are obtained by numerically integrating (98-100) and the dashed lines are obtained using (113). It is clear that (113) yields a good approximation to E_{max} for large γ .

In order to compare (113) to expressions for E_{max} obtained elsewhere [10–12], it is useful to express (113) as a function of effective temperature. The electron proper number density $n = n_{\text{ion}}$ when $\mu = \mu_{\text{eq}}$ and we eliminate b in favour of an effective longitudinal temperature $T_{\parallel\text{eq}}$ defined as

$$T_{\parallel\text{eq}} = \frac{1}{k_B n_{\text{ion}}} p_{\parallel\text{eq}} \tag{114}$$

where k_B is Boltzmann's constant and $p_{\parallel\text{eq}}$ is the longitudinal pressure associated with the oscillator equilibrium $\mu = \mu_{\text{eq}}$. The longitudinal pressure is $p_{\parallel\text{eq}} = \mathcal{T}_{\text{eq}}^{33}$ where the stress-energy-momentum tensor \mathcal{T}_{eq} has components

$$\mathcal{T}_{\text{eq}}^{ab} = m\alpha \int_{\mathcal{W}_{\text{eq}}} \dot{x}^a \dot{x}^b \iota_X \#1 \tag{115}$$

with \mathcal{W}_{eq} the support of the waterbag distribution $\mu = \mu_{\text{eq}}$ (the choice of fibre is unimportant as the distribution associated with μ_{eq} is independent of ζ).

Since

$$\frac{\dot{x}^{32} d\dot{x}^1 \wedge d\dot{x}^2 \wedge d\dot{x}^3}{\sqrt{\beta^2 + \dot{x}^{32}}} = d \left\{ \left[\frac{1}{2} \dot{x}^3 \sqrt{\beta^2 + \dot{x}^{32}} - \frac{1}{2} \beta^2 \sinh^{-1} \left(\frac{\dot{x}^3}{\beta} \right) \right] d\dot{x}^1 \wedge d\dot{x}^2 \right\} \tag{116}$$

where $\dot{x}^{12} \equiv (\dot{x}^1)^2$, $\dot{x}^{22} \equiv (\dot{x}^2)^2$, $\dot{x}^{32} \equiv (\dot{x}^3)^2$ and $\beta \equiv \sqrt{1 + \dot{x}^{12} + \dot{x}^{22}}$, using (115) and Stokes' theorem on forms, it follows

$$\mathcal{T}_{\text{eq}}^{33} = m\alpha \int_{\partial\mathcal{W}_{\text{eq}}} \left[\frac{1}{2} \dot{x}^3 \sqrt{\beta^2 + \dot{x}^{32}} - \frac{1}{2} \beta^2 \sinh^{-1} \left(\frac{\dot{x}^3}{\beta} \right) \right] d\dot{x}^1 \wedge d\dot{x}^2. \tag{117}$$

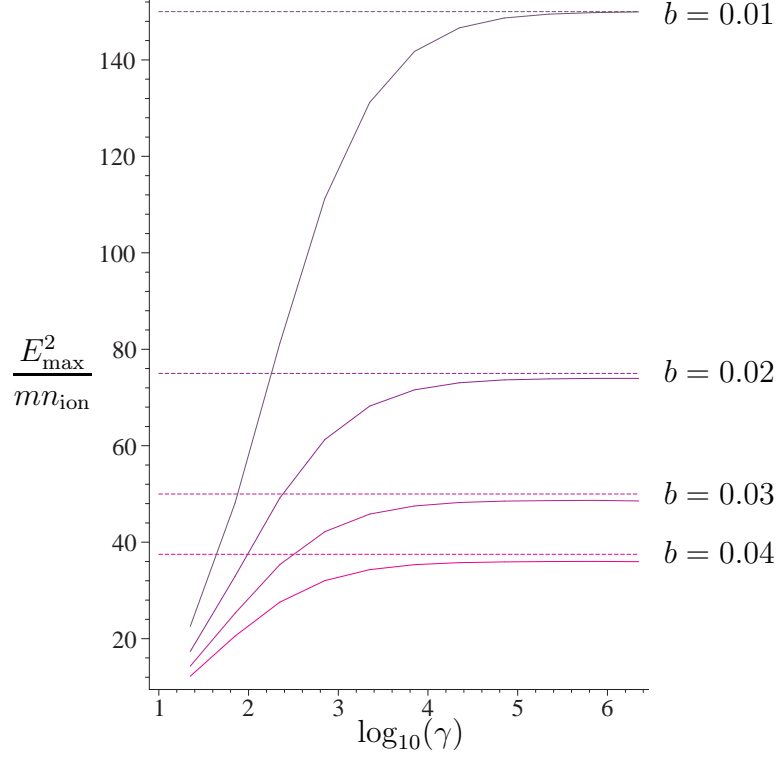


Figure 4: $E_{\max}^2/(mn_{\text{ion}})$ versus $\log_{10}(\gamma)$ for $R = 0.2$ and $b \in \{0.01, 0.02, 0.03, 0.04\}$. The dashed lines are the approximation (113) and the solid curves are obtained by numerically integrating (98-100).

Using (79, 80), components of the oscillator equilibrium waterbag $\dot{x}^a = V_{\xi^a}^a$ are

$$\dot{x}^0 = \mu_{\text{eq}} - a \cos(\xi^1) - v \sqrt{[\mu_{\text{eq}} - a \cos(\xi^1)]^2 - \gamma^2[1 + R^2 \sin^2(\xi^1)]}, \quad (118)$$

$$\dot{x}^1 = R \sin(\xi^1) \cos(\xi^2), \quad (119)$$

$$\dot{x}^2 = R \sin(\xi^1) \sin(\xi^2), \quad (120)$$

$$\dot{x}^3 = v[\mu_{\text{eq}} - a \cos(\xi^1)] - \sqrt{[\mu_{\text{eq}} - a \cos(\xi^1)]^2 - \gamma^2[1 + R^2 \sin^2(\xi^1)]} \quad (121)$$

and it follows

$$\begin{aligned} \frac{\dot{x}^3}{a} &= v[\hat{\mu}_{\text{eq}} - \cos(\xi^1)] - \sqrt{[\hat{\mu}_{\text{eq}} - \cos(\xi^1)]^2 - \varepsilon^2[1 + R^2 \sin^2(\xi^1)]} \\ &\approx \left(-\frac{1}{2}b^2[\hat{\mu}_{\text{eq}}(0) - \cos(\xi^1)] + \frac{1}{2[\hat{\mu}_{\text{eq}}(0) - \cos(\xi^1)]} \right) \varepsilon^2 \end{aligned} \quad (122)$$

to lowest order in ε and R . Using (109, 122) it follows

$$\frac{\dot{x}^3}{a} \approx \varepsilon^2 b^2 \cos(\xi^1) \quad (123)$$

to lowest order in ε , b and R . Furthermore, (102, 107) yield $a\varepsilon^2 b^2 = b/v \approx b$ and so

$$\dot{x}^3 \approx b \cos(\xi^1) \quad (124)$$

to lowest order in ε , b and R . Hence

$$\frac{\dot{x}^3}{2} \sqrt{\beta^2 + \dot{x}^{32}} - \frac{1}{2}\beta^2 \sinh^{-1} \left(\frac{\dot{x}^3}{\beta} \right) \approx \frac{1}{3}b^3 \cos^3(\xi^1) \quad (125)$$

to lowest order in ε , b and R and (117) yields

$$\begin{aligned} p_{\parallel\text{eq}} &\approx \frac{4\pi m\alpha R^2 b^3}{15} \\ &= \frac{1}{5} m n_{\text{ion}} b^2. \end{aligned} \tag{126}$$

Equations (113, 114, 126) yield

$$E_{\text{max}}^2 \approx \frac{m^2 \omega_p^2 c^2}{q^2} \left(\frac{9mc^2}{20k_B T_{\parallel\text{eq}}} \right)^{1/2}, \quad \varepsilon, b, R \ll 1 \tag{127}$$

where $\omega_p = \sqrt{n_{\text{ion}} q^2 / (m\varepsilon_0)}$ is the plasma frequency and the speed of light c and permittivity of the vacuum ε_0 have been restored.

Conclusion

Equations (78, 127) indicate that waterbags over 2-dimensional spacetime and 4-dimensional spacetime can behave quite differently. Equation (127) is independent of γ but (78) diverges as $\gamma \rightarrow \infty$, and this difference in behaviour arises because the logarithmic singularity in the integrand in (113) is integrable. Moreover, the $T_{\parallel\text{eq}}^{-1/4}$ behaviour of the asymptotic form of E_{max} for $k_B T_{\parallel\text{eq}} \ll mc^2$ is very similar to the results of SES [12] and others [11] in the limit $v \rightarrow c$.

Direct comparison of our results and those of SES follows by setting the transverse vector potential \mathbf{A}_{\perp} to zero in the SES model, thereby neglecting the overlap of the electromagnetic field of the driver (laser pulse or particle bunch) and the wave. The approach followed by SES begins with covariant field equations, induced from the Vlasov equation, that couple the zeroth, first and second order centred moments (in \dot{x}^a) of the 1-particle distribution f with the electromagnetic field. SES then assume that the 1-particle distribution f (restricted by pull-back to the unit hyperboloid) may be approximated as³ $f \simeq h(x^0, x^3, \dot{x}^3) \delta(\dot{x}^1) \delta(\dot{x}^2)$ where δ is the Dirac delta function. A covariant measure of the total thermal spread is given by the magnitude ϵ^2 of the ratio of the trace of the second order centred moment and the zeroth moment. SES assume that the third order centred moment is $\mathcal{O}(\epsilon^3)$ and can be neglected relative to lower order moments.

One could develop a similar argument to that given by SES based on moments of a prescribed 3-dimensional waterbag with narrow velocity spread, rather than the line distribution employed by SES. However, nuances in the shape of the waterbag would be lost; for example, we would not know that merely the tip of the waterbag grazes the wave's phase velocity (see figure 3) during the maximum amplitude oscillation. This could be important because, as noted earlier, longitudinal wave-breaking is associated with the trapping of considerable numbers of particles in the wave (see [15] for a discussion), and our present model neglects trapped particles. Thus, we expect that E_{max} calculated here is a lower bound on the maximum electric field obtained when trapping is accounted for.

In conclusion, we have shown that it is possible to construct 3-dimensional waterbag distributions that lead to a maximum electric field amplitude whose asymptotic behaviour is similar to that of the SES model as $v \rightarrow c$ (with effective temperature held fixed in the limit $v \rightarrow c$).

Acknowledgements

We thank RMGM Trines for useful discussions. We acknowledge EPSRC for financial support.

References

- [1] T Tajima and JM Dawson, Phys. Rev. Lett. 43 (1979) 267
- [2] P Chen, *et al.*, Phys. Rev. Lett. 54 (1985) 693
- [3] V Malka, *et al.*, Nat. Phys. 4 (2008) 447

³We have changed the notation used by SES to avoid conflict with our own.

- [4] A Caldwell, *et al.*, Nat. Phys. 5 (2009) 363
- [5] W Wuensch, Proc. EPAC 2002 134
- [6] HP Schlenvoigt, *et al.*, Nat. Phys. 4 (2008) 133
- [7] AI Akhiezer and RV Polovin, Sov. Phys. JETP 3 (1956) 696
- [8] JM Dawson, Phys. Rev. 113 (1959) 383
- [9] TP Coffey, Phys. Fluids 14 (1971) 1402
- [10] T Katsouleas and WB Mori, Phys. Rev. Lett. 61 (1988) 90
- [11] JB Rosenzweig, Phys. Rev. A 38 (1988) 3634
- [12] CB Schroeder, E Esarey and BA Shadwick, Phys. Rev. E 72 (2005) 055401
- [13] RMGM Trines and PA Norreys, Phys. Plasmas 13 (2006) 123102
- [14] CB Schroeder, E Esarey and BA Shadwick, Phys. Plasmas 14 (2007) 084701
- [15] RMGM Trines and PA Norreys, Phys. Plasmas 14 (2007) 084702
- [16] SPD Mangles, *et al.*, Nature 431 (2004) 535–8
- [17] CGR Geddes, *et al.*, Nature 431 (2004) 538–41
- [18] J Faure, *et al.*, Nature 431 (2004) 541–4
- [19] W Lu, *et al.*, Phys. Plas. 13 (2006), 056709
- [20] T Esirkepov, *et al.*, Phys. Rev. Lett. 96 (2006) 014803
- [21] WB Mori and T Katsouleas, Phys. Scr. T30 (1990) 127
- [22] DA Burton and A Noble, AIP Conf. Proc. 1086 (2009) 252
- [23] DA Burton, A Noble and H Wen, Il Nuovo Cim. C 32 1 (2009) 1
- [24] J Ehlers in *General Relativity and Cosmology*, Proceedings of the International School of Physics “Enrico Fermi” 47, (Academic Press, New York and London, 1971) 1
- [25] DA Burton, Theoret. Appl. Mech. 30 (2003) 85
- [26] IM Benn and RW Tucker, *An Introduction to Spinors and Geometry with Applications in Physics* (Adam Hilger, Bristol and New York, 1987)